

First-forbidden mirror β -decays in $A = 17$ mass region

N. Michel[†], J. Okołowicz^{†§}, F. Nowacki[‡], and M. Płoszajczak^{†©}

[†] *Grand Accélérateur National d'Ions Lourds (GANIL), CEA/DSM – CNRS/IN2P3, BP 5027,*

F-14076 Caen Cedex 05, France

[§] *Institute of Nuclear Physics, Radzikowskiego 152, PL - 31342 Krakow, Poland*

[‡] *Laboratoire de Physique Théorique Strasbourg (EP 106), 3-5 rue de l'Université, F-67084*

Strasbourg Cedex, France

[©] *Institute for Nuclear Theory, University of Washington, Box 351550, Seattle, WA 98195, USA*

Abstract

The first-forbidden β -decay of ^{17}Ne into the 'halo' state $J^\pi = 1/2_1^+$ of ^{17}F presents one of the largest measured asymmetries for mirror β -decay feeding bound final states. This asymmetry is studied in the framework of the Shell Model Embedded in the Continuum (SMEC). The spatial extent of single particle orbits is constrained by the proton capture cross-section $^{16}\text{O}(p, \gamma)^{17}\text{F}$ calculated in SMEC. This allows to estimate mirror symmetry breaking in $^{17}\text{F}/^{17}\text{O}$ and $^{17}\text{Ne}/^{17}\text{N}$ nuclei.

21.60.Cs, 23.40.-s, 23.40.Hc, 25.40.Lw

I. INTRODUCTION

A realistic account of the low-lying states properties in exotic nuclei requires taking into account the coupling between discrete and continuum states which is responsible for unusual spatial features of these nuclei. This aspect is particularly important in the studies near drip line where the amount of experimental information is strongly reduced and one has to use both structure and reaction data to understand basic properties of these nuclei. Within the Shell Model Embedded in the Continuum (SMEC) approach [1,2], one may obtain the unified description of the divergent characteristics such as the spectra (energies of states, transition probabilities, proton/neutron emission widths, β -decays, etc.) and the reactions involving one-nucleon in the continuum (proton/neutron capture processes, Coulomb dissociation reactions, elastic/inelastic proton/neutron reactions, etc.). This provides a stringent test of the effective interactions in the SMEC calculations and permits to assess the mutual complementarity of reaction and structure data for the understanding of these nuclei. In this context, it can be interesting to compare the first-forbidden β -decay transition of ^{17}Ne in the ground state (g.s.) $J^\pi = 1/2_1^-$ to the weakly bound, first excited state $J^\pi = 1/2_1^+$ in ^{17}F , with the corresponding mirror decay of ^{17}N into a well bound excited state of ^{17}O . In these decays an abnormal asymmetry of mirror decay rates has been observed by Borge et al. [3] and later confirmed by Ozawa et al. [4]. Borge et al. [3] explained this effect by the large asymmetry of radial sizes of $s_{1/2}$ s.p. orbits involved in bound states of $^{17}\text{F}/^{17}\text{O}$ and $^{17}\text{Ne}/^{17}\text{N}$. Different explanation has been provided by Millener [5] who attributes the bulk of the asymmetry to charge dependent effects which lead to different $1s_{1/2}$ occupancy for the initial states, *i.e.* to different amplitudes of $\pi(0p_{1/2}^2 1s_{1/2}^2)\nu(0p_{1/2}^1)$ and $\nu(0p_{1/2}^2 1s_{1/2}^2)\pi(0p_{1/2}^1)$ components in the g.s. of ^{17}Ne and ^{17}N , respectively.

In the framework of SMEC, we shall discuss the constraints from proton capture cross-section data on the radial wave function involved in the description of the first-forbidden β -decay into bound final states.

In the SMEC formalism, which derives from the continuum shell model formalism [6,7], the subspaces of (quasi-) bound (the Q subspace) and scattering (the P subspace) states are separated using the projection operator technique. P subspace contains asymptotic channels, which are made of $(N - 1)$ -particle localized states and one nucleon in the scattering state, whereas Q subspace contains many-body localized states which are build up by the bound single-particle (s.p.) wave functions and by the s.p. resonance wave functions. The wave functions in Q and P are then properly renormalized in order to ensure the orthogonality of wave functions in both subspaces.

In the first step, we calculate the (quasi-) bound many-body states in Q subspace. For that we solve the multiconfigurational Shell Model (SM) problem : $H_{QQ}\Phi_i = E_i\Phi_i$, where H_{QQ} is given by the SM effective interaction which is responsible for the *internal mixing* of many-body configurations. The quality of the SMEC description depends crucially on the realistic account of configuration mixing for the coexisting low-lying structures and hence on the quality of the SM effective interactions and the SM space considered. In the description of $A = 17$ nuclei, it is important to take into account the dynamics of ^{16}O core and to include 2p-2h and 4p-4h excitation from p -shell to sd - shell. Zuker-Buck-McGrory (ZBM) effective SM interaction in the basis of $0p_{1/2}$, $1s_{1/2}$ and $0d_{5/2}$ orbitals [8,9], allows to take into account this dynamics. The valence space $(0p_{1/2}, 1s_{1/2}, 0d_{5/2})$ has the advantage to be

practically non spurious and most of states at the $p-sd$ interface are well described through the configuration mixing of these three orbitals. Results of this paper have been obtained with the ZBM interaction.

II. DETAILS OF THE MODEL

To generate the radial s.p. wave functions in Q subspace and the scattering wave functions in P subspace, as a first guess, we use the average potential of Woods-Saxon (WS) type with the spin-orbit : $V_{SO}\lambda_\pi^2(2\mathbf{l}\cdot\mathbf{s})r^{-1}df(r)/dr$, and Coulomb parts included. $\lambda_\pi^2 = 2\text{ fm}^2$ is the pion Compton wavelength and $f(r)$ is the spherically symmetrical WS formfactor. The Coulomb potential V_C is calculated for the uniformly charged sphere of radius R_0 (see Table 1). This 'first guess' potential $U(r)$, is then modified by the residual interaction. We shall return to this problem below.

For the continuum part, we solve the coupled channel equations :

$$(E - H_{PP})\xi_E^{(+)} \equiv \sum_{c'} (E - H_{cc'})\xi_E^{c'+(+)} = 0 \quad , \quad (1)$$

where index c denotes different channels and $H_{PP} \equiv PHP$. The superscript (+) means that boundary conditions for incoming wave in the channel c and outgoing scattering waves in all channels are used. The channel states are defined by coupling of one nucleon in the scattering continuum to the many-body SM state in $(N - 1)$ -nucleus. For the coupling between bound and scattering states around ^{16}O , we use the density dependent interaction (DDSM1) [10,11]. This interaction provides *external mixing* of SM configurations via the virtual excitations of particles to the continuum states. The channel - channel coupling potential : $H_{cc'} = (T + U)\delta_{cc'} + v_{cc'}^J$, contains the kinetic-energy operator T and the channel-channel coupling $v_{cc'}^J$ generated by the residual interaction. At a first step, the potential for channel c consists of the initial WS potential $U(r)$, and of the diagonal part of coupling potential v_{cc}^J which depends on both the s.p. orbit $\phi_{l,j}$ and the considered many-body state J . Hence, the initial potential is modified by the coupling potential and in the next step the s.p. wave functions $\phi_{l,j}$ defining Q subspace are generated by the modified potential, what in turn modifies the diagonal part of the residual force, *etc.* In other words, the procedure of solving coupled channel equations (1) is accompanied by the self-consistent iterative procedure which for each total J yields the J -dependent self-consistent potential : $U^{(sc)}(r) = U(r) + v_{cc}^{J(sc)}(r)$, and consistent with it the new renormalized formfactor of the coupling force. $U^{(sc)}(r)$ differs significantly from the initial potential, especially in the interior of the potential [2,10]. For weakly bound many-body states, strong modification of the surface features of the initial potential $U(r)$ has been found as well [2,10]. Parameters of the first guess potential $U(r)$ are such that $U^{(sc)}(r)$ reproduces energies of experimental s.p. states, whenever their identification is possible. For certain J , the s.p. wave functions are not modified by the above iterative procedure. For example in $J^\pi = 1/2^+$ states of ^{17}F and ^{17}O , the couplings to the g.s. 0^+ of ^{16}O modify only $1s_{1/2}$ s.p. wave function. In this case, the radial wave functions of all other s.p. states are generated by an auxiliary average potential $U^{(aux)}(r)$ of the WS type with spin-orbit and Coulomb parts included. We shall return to this problem below.

The third system of equations in SMEC consists of the inhomogeneous coupled channel equations:

$$(E^{(+)} - H_{PP})\omega_i^{(+)} = H_{PQ}\Phi_i \equiv w_i \quad . \quad (2)$$

The source term w_i depends on the structure of N - particle SM wave function Φ_i . The radial formfactor of the source depends on s.p. wave functions of $U(r)$ ($U^{(aux)}(r)$). Solutions of the eqs. (2) describe the decay of quasi-bound state Φ_i in the continuum. Reduced matrix elements of the source term involve products of two annihilation operators and one creation operator : $\mathcal{R}_{\gamma\delta(L)\beta}^{j\alpha} = (a_{\beta}^{\dagger}(\tilde{a}_{\gamma}\tilde{a}_{\delta})^L)^{j\alpha}$. In the SMEC calculations for ^{17}F and ^{17}O , the matrix elements of the source term depend sensitively on the percentage of the shell closure in ^{16}O , *i.e.*, on the amount of correlations both in the g.s. of ^{16}O and in the considered states of ^{17}F or ^{17}O [11]. The total wave function is expressed by three functions: Φ_i , ξ_E^c and ω_i [7,1,2] :

$$\Psi_E^c = \xi_E^c + \sum_{i,j} (\Phi_i + \omega_i) \frac{1}{E - H_{QQ}^{eff}} \langle \tilde{\Phi}_j | H_{QP} | \xi_E^c \rangle \quad (3)$$

where :

$$H_{QQ}^{eff}(E) = H_{QQ} + H_{QP}G_P^{(+)}H_{PQ} \quad , \quad (4)$$

is the energy dependent effective SM Hamiltonian in Q subspace which contains couplings to the continuum. Operator $H_{QQ}^{eff}(E)$ is hermitian for energies below the particle emission threshold and non-hermitian for energies higher than the threshold. The eigenvalues $\tilde{E}_i - \frac{1}{2}i\tilde{\Gamma}_i$ are complex for decaying states and depend on the energy E of the particle in the continuum. The energy and the width of resonance states are determined by the condition: $\tilde{E}_i(E) = E$. The eigenstates corresponding to these eigenvalues can be obtained by the orthogonal but in general non-unitary transformation [1,2,6,7]. Inserting them in (3), one obtains symmetrically the new continuum many-body wave function modified by the discrete states :

$$\Psi_E^c = \xi_E^c + \sum_i \tilde{\Omega}_i \frac{1}{E - \tilde{E}_i + (i/2)\tilde{\Gamma}_i} \langle \tilde{\Phi}_i | H | \xi_E^c \rangle \quad , \quad (5)$$

and the new discrete state wave function modified by the coupling to the continuum states:

$$\tilde{\Omega}_i = \tilde{\Phi}_i + \sum_c \int_{\epsilon_c}^{\infty} dE' \xi_{E'}^c \frac{1}{E^{(+)} - E'} \langle \xi_{E'}^c | H | \tilde{\Phi}_i \rangle \quad . \quad (6)$$

These SMEC wave functions will be used in this paper to calculate spectra of ^{17}F , ^{17}O , the first-forbidden β -decays : $^{17}\text{Ne}(\beta^+)^{17}\text{F}$, $^{17}\text{N}(\beta^-)^{17}\text{O}$, and the radiative proton capture reaction $^{16}\text{O}(p,\gamma)^{17}\text{F}$.

Figs. 1 and 2 show SMEC energies and widths for positive parity (l.h.s. of the plot) and negative parity (r.h.s. of the plot) states of ^{17}F and ^{17}O , respectively. Large breaking of mirror symmetry, which can be seen by comparing spectra in Figs. 1 and 2, is due to the combined effect of the low separation energy and the Coulomb field. The continuum coupling, which due to different positions of the lowest particle emission thresholds acts

differently in ^{17}F and ^{17}O , cannot fully account for the observed mirror symmetry breaking. The simplest way of correcting this deficiency is to adjust the spacing of $d_{5/2}$ and $s_{1/2}$ s.p. orbitals in ZBM interaction in such a way that the experimental energy splitting between the g.s. $5/2_1^+$ and the first excited state $1/2_1^+$ in ^{17}O and ^{17}F is reproduced by the SMEC calculation. In this way, the s.p. energy of $d_{5/2}$ in ZBM interaction becomes : $\varepsilon_{d_{5/2}} = 3.95$ and 3.5 in ^{17}F and ^{17}O , respectively. The energy of $s_{1/2}$ orbital remains $\varepsilon_{s_{1/2}} = 3.3$ in both cases. In the following, these two hybrid interactions will be called ZBM-F and ZBM-O interactions , respectively. The Thomas-Ehrmann shift is then taken into account through the combined effect of the mirror symmetry breaking continuum coupling and the modification of the s.p. energies of the effective SM interaction.

The coupling matrix elements between the $J^\pi = 0_1^+$ g.s. wave function of ^{16}O and all considered states in ^{17}F and ^{17}O are calculated using the density dependent DDSM1 interaction [10,11]. The coupling to the continuum states is given by the matrix elements of $\mathcal{R}_{\gamma\delta(L)\beta}^{j\alpha}$ between g.s. of ^{16}O and all considered states in ^{17}F and ^{17}O . The calculation of the radial wave functions and radial formfactors of the coupling to the continuum states goes as follows. The s.p. wave functions, which in the many body states J^π of ^{17}F are not modified by the selfconsistent correction to the finite initial potential, are calculated using the auxiliary potential $U^{(aux)}$. This potential, which contains central , spin-orbit and Coulomb parts, is adjusted to yield the binding energies of proton s.p. orbits $0d_{5/2}$ and $1s_{1/2}$ at the experimental binding energies of $5/2_1^+$ and $1/2_1^+$ states in ^{17}F . This adjustment of binding energies of s.p. orbits makes sense because the many-body wave function $5/2_1^+$ (respectively $1/2_1^+$) has a large amplitude of the component with one particle in $0d_{5/2}$ (respectively $1s_{1/2}$) s.p. state outside of the ^{16}O core. The parameters of this potential are given in Table 1 for different values of the diffuseness parameter a . Without Coulomb term, the same potential is used also to calculate radial formfactors for neutrons in ^{17}F . In the calculation for ^{17}O , again the same potential with the Coulomb term of ^{17}O is used. Such a potential yields binding energies of neutron $0d_{5/2}$ and $1s_{1/2}$ s.p. orbits very closely to the experimental binding energies of $5/2_1^+$ and $1/2_1^+$ states in ^{17}O . If the coupling between bound and scattering states modifies the s.p. wave function $\phi_{l,j}$ in the many body state J^π , then the depth of the initial potential $U(r)$ is readjusted to ensure that the energy of the s.p. state $\phi_{l,j}$ in the selfconsistent potential $U^{(sc)}(r)$ is the same as the energy of this state in the auxiliary potential $U^{(aux)}$. The remaining parameters : R_0 , a , V_{SO} , of the initial potential are the same as in $U^{(aux)}$. This procedure for radial wave functions yields the same asymptotic property for a given s.p wave function in all different channels.

The calculation of the first-forbidden β -decays presented in this work are the extension of the calculations of Towner and Hardy [12] (see also Ref. [13] for the presentation of the method). In the following we give only few elements of this approach to introduce the notation used in this work. The calculation of the absolute decay rate uses [14,15] : $f t_{1/2} = 6170$ s, where $t_{1/2}$ is the partial half-life and :

$$f = \int_1^{W_0} C(W)F(Z,W)(W^2 - 1)^{1/2}W(W_0 - W)^2dW . \quad (7)$$

In the above expression, W is the β -energy, W_0 is the maximum β -energy and Z is the charge of the final nucleus. The first-forbidden shape factor $C(W)$ can be written to a good approximation as [14,12] : $C(W) = k(1 + aW + bW^{-1} + cW^2)$, where coefficients k , a , b and

c depend on the nuclear matrix elements, W_0 and $\xi = Ze^2/2R$. (For the nuclear radius R we use the prescription of Wilkinson [15].) Consequently :

$$f = k(I_0 + aI_1 + bI_{-1} + cI_2) . \quad (8)$$

The evaluation of integrals I_k is given in [16]. Relation of the coefficients k, a, b, c to the nuclear matrix elements of different rank is [14,17] :

$$\begin{aligned} k &= \left[\zeta_0^2 + \frac{1}{9}w^2 \right]^{(0)} + \\ &+ \left[\zeta_1^2 + \frac{1}{9}(x+u)^2 - \frac{4}{9}\mu_1\gamma_1u(x+u) + \frac{1}{18}W_0^2(2x+u)^2 - \frac{1}{18}\lambda_2(2x-u)^2 \right]^{(1)} + \\ &+ \frac{1}{12} \left[z^2(W_0^2 - \lambda_2) \right]^{(2)} , \\ ka &= - \left[\frac{4}{3}uY - \frac{1}{9}W_0(4x^2 + 5u^2) \right]^{(1)} - \left[\frac{1}{6}z^2W_0 \right]^{(2)} , \\ kb &= \frac{2}{3}\mu_1\gamma_1 \{ -[\zeta_0w]^{(0)} + [\zeta_1(x+u)]^{(1)} \} , \\ kc &= \frac{1}{18} [8u^2 + (2x+u)^2 + \lambda_2(2x-u)^2]^{(1)} + \left[\frac{1}{12}z^2(1 + \lambda_2) \right]^{(2)} , \end{aligned} \quad (9)$$

where

$$\begin{aligned} V &= \xi'v + \xi w' , & \zeta_0 &= V + \frac{1}{3}wW_0 , \\ Y &= \xi'y - \xi(u' + x') , & \zeta_1 &= Y + \frac{1}{3}(u-x)W_0 . \end{aligned}$$

The quantities μ_1, γ_1 and λ_2 are defined in terms of the electron wave functions and have values close to unity [14]. The non-relativistic form of the nuclear matrix elements is [17] :

$$\begin{aligned} w &= \lambda\sqrt{3}\langle J_f T_f || ir[\mathbf{C}_1 \times \sigma]^0 \tau || J_i T_i \rangle C , \\ x &= -\langle J_f T_f || ir\mathbf{C}_1 \cdot \tau || J_i T_i \rangle C , \\ u &= \lambda\sqrt{2}\langle J_f T_f || ir[\mathbf{C}_1 \times \sigma]^1 \tau || J_i T_i \rangle C , \\ z &= -2\lambda\langle J_f T_f || ir[\mathbf{C}_1 \times \sigma]^2 \tau || J_i T_i \rangle C , \end{aligned} \quad (10)$$

where $\lambda = -g_A/g_V = 1.2599(25)$ [18] and :

$$C = \frac{\langle T_i T_{z_i} 1 \pm 1 | T_f T_{z_f} \rangle}{[2(2J_i + 1)(2T_f + 1)]^{1/2}} \quad (11)$$

The remaining matrix elements in the non-relativistic form are :

$$\begin{aligned} \xi'v &= -\lambda\sqrt{3}\langle J_f T_f || \frac{i}{M}[\sigma \times \nabla]^0 \tau || J_i T_i \rangle C , \\ \xi'y &= \langle J_f T_f || \frac{i}{M}\nabla \cdot \tau || J_i T_i \rangle C , \end{aligned} \quad (12)$$

where M is the nucleon mass. It has been found by Warburton et al. [19,20] that the matrix element $\xi'v$ of the time-like piece of the axial current is strongly enhanced by meson-exchange currents, mainly the one-pion exchange. The enhancement factor that multiplies the impulse-approximation axial-charge matrix element, has been determined by comparison to experiment for $A \sim 16$ to be $\epsilon = 1.61 \pm 0.03$. In all calculations discussed in this work, we multiply the matrix element $\xi'v$ by a constant factor 1.61, like in the analysis of Borge et al. [3]. Somewhat smaller enhancement factor has been used in the study of Millener [5]. This meson exchange contribution to the axial charge is very important, changing the absolute decay rates of the first-forbidden decays f^- and f^+ by a factor ~ 3.7 (see also the discussion in [5]). However, its influence on the ratio f^+/f^- is somewhat less important.

The matrix elements w', x' and u' are obtained from w, x and u by including an extra factor in the radial integral [17]. For the higher energy part of the spectrum in light nuclei, the term kbW^{-1} can be neglected and the energy dependence of $C(W)$ is determined entirely by the matrix elements of multipolarity 1 and 2 [12], *i.e.* by ka and kc . As written above, the expressions for the matrix elements apply to electron emission. For positron emission we have to make the following replacement : $Z \rightarrow -Z$ and $\lambda \rightarrow -\lambda$. Even assuming perfect mirror symmetry, the nuclear matrix elements combine in f with different signs what gives a different shape correction factor for electron and positron decays. The evaluation of matrix elements in the basis of selfconsistently determined s.p. wave functions in the initial $J_i^\pi = 1/2^-$ and final $J_f^\pi = 1/2^+$ many body states follows the procedure described by Towner and Hardy [12] and adopted in Ref. [3].

III. DISCUSSION

An exceptionally large asymmetry of mirror β -decays : $^{17}\text{N}(J^\pi = 1/2_1^-) \rightarrow ^{17}\text{O}(J^\pi = 1/2_1^+)$ and $^{17}\text{Ne}(J^\pi = 1/2_1^-) \rightarrow ^{17}\text{F}(J^\pi = 1/2_1^+)$, raises the question about a role of largely different radial sizes of $1s_{1/2}$ s.p. wave functions in the initial state $1/2_1^-$ of $^{17}\text{Ne}/^{17}\text{N}$. In the final state $1/2_1^+$, the large asymmetry of radial configurations of ^{17}F , ^{17}O and the halo structure of the ^{17}F is well known. A dominant component of the $1/2_1^-$ wavefunction in $^{17}\text{Ne}/^{17}\text{N}$ is $\pi(0d_{5/2}^2)\nu(0p_{1/2}^{-1})/\nu(0d_{5/2}^2)\pi(0p_{1/2}^{-1})$ configuration outside the core of ^{16}O but this configuration does not play a role in the first-forbidden β -decay. The dominant contribution comes from the small component of the wave function $\pi(1s_{1/2}^2)\nu(0p_{1/2}^{-1})/\pi(1s_{1/2}^2)\nu(0p_{1/2}^{-1})$ in the g.s. of $^{17}\text{Ne}/^{17}\text{N}$. For this component, $1s_{1/2}$ nucleon makes a transition to fill the $0p_{1/2}$ hole.

Assuming strict mirror symmetry in the β -decays, the SM analysis yields the ratio f^+/f^- which is much smaller ($f^+/f^- \simeq 9.6$) than the experimental value (24 ± 4) [3]. Allowing for the variation of radii of selected s.p. orbits, Borge et al. [3] have shown that the observed values of the ratio f^+/f^- can be reproduced in the SM analysis assuming a difference of ~ 0.6 fm between the oscillator length parameters for proton and neutron $1s_{1/2}$ orbitals. It was assumed that radii of $1s_{1/2}$ neutron orbits in ^{17}N and ^{17}O are the same. Similar assumption has been made for radii of $1s_{1/2}$ proton orbits in ^{17}Ne and in ^{17}F . Remaining s.p. orbits have been assumed to have the same radius in ^{17}F , ^{17}Ne , ^{17}O and ^{17}N .

High sensitivity of the β -decay asymmetry to the spatial features of s.p. orbits [3], provides a challenge for the SMEC approach because radial characteristics for certain orbits as well as their asymptotic properties are determined consistently for each studied nu-

cleus and, moreover, model parameters (the effective SM interaction, the residual coupling, radius/diffuseness of the initial/auxiliary average potential) are determined by analyzing different reaction and spectroscopic data in the same many-body framework.

In Fig. 3 we show f^+ , f^- and f^+/f^- , which are calculated in SMEC for different values of the diffuseness parameter of the initial potential. In each case, the same diffuseness is taken for initial potentials in ^{17}Ne , ^{17}N , ^{17}F and ^{17}O . The shaded areas show the experimental limits for these values. f^+ and f^- are calculated with ZBM-F and ZBM-O interactions (the solid lines), respectively. The dotted line in the middle part of Fig. 3 shows results for f^- obtained with ZBM-F interaction. The corresponding ratio f^+/f^- , shown by the dotted line in the lower part of Fig. 3, corresponds then to strictly mirror symmetric SM interaction. The coupling to continuum is given by DDSM1 residual interaction in all studied cases. The calculations of the radial wave functions and radial formfactors of the coupling to the continuum states for $^{17}\text{F}/^{17}\text{O}$ have been described above. In the calculations for $^{17}\text{Ne}/^{17}\text{N}$, we employed the initial/auxiliary potentials obtained from those for $^{17}\text{F}/^{17}\text{O}$ by an appropriate modification of the Coulomb potential. One should mention, that initial potentials $U(r)$ ($U^{(aux)}(r)$) for different diffuseness parameters, yield very similar spectra for each considered nucleus. Therefore, the energy spectra do not provide any constraint on the diffuseness of the average field. The experimental value of the ratio f^+/f^- can be reproduced using $U(r)$ ($U^{(aux)}(r)$) with a very large value of the diffuseness parameter ($a \sim 0.8$ fm). However, none of these potentials with extremely thick skin can reproduce the experimental values for either f^+ ($f_{exp}^+ = 927 \pm 95$) or f^- ($f_{exp}^- = 44 \pm 7$).

The overall contribution of matrix elements of rank 1 in f^+ and f^- increases with increasing diffuseness parameter from $\sim 11\%$ at $a = 0.4$ fm to $\sim 21\%$ at $a = 0.8$ fm. This strong relative increase is similar for f^+ and f^- . More insight into the a -dependence of f^+ and f^- can be gained from Fig. 4 (see also Tables 2 and 3) which shows the matrix elements : kI_0 (the upper part) and the sum $kaI_1 + kcI_2$, separately for $^{17}\text{Ne}(\beta^+)^{17}\text{F}$ (the solid lines) and $^{17}\text{N}(\beta^-)^{17}\text{O}$ (the dotted lines) decays. kI_0 is the combination of nuclear matrix elements of rank 0 and 1. Coefficient k is the energy-independent term of the first-forbidden shape factor $C(W)$. The sum of kaI_1 and kcI_2 depends on nuclear matrix elements of rank 1 only. In our case, the nuclear matrix elements of rank 2 associated with the operator z^2 (*c.f.* equation (9)) are identically equal zero. The coefficients ka and kc determine W - and W^2 -dependence of the shape correction factor $C(W)$. ZBM-F and ZBM-O interactions are used in the calculation of β^+ and β^- decays respectively. $(kI_0)^+$ and $(kI_0)^-$ decrease with increasing a and the decrease rate is similar in both cases. The strong increase of the ratio f^+/f^- for large a is caused by a different a -dependence of $(kaI_1 + kcI_2)^+$ and $(kaI_1 + kcI_2)^-$. With increasing diffuseness of $U(r)$ ($U^{(aux)}(r)$), $(kaI_1 + kcI_2)^+$ decreases strongly whereas $(kaI_1 + kcI_2)^-$ remains approximately constant and is negative. In the studied range of a values, the ratio $(kI_0)^+/(kI_0)^-$ increases only by $\sim 25\%$ whereas $[(kI_0)^+ + (kaI_1 + kcI_2)^+]/[(kI_0)^- + (kaI_1 + kcI_2)^-] \simeq f^+/f^-$ increases by $\sim 70\%$. At the same time, kbI_{-1} is small and almost constant. Hence, those nuclear matrix elements of multipolarity 1 which determine the β -energy dependence of the first-forbidden shape factor play also a salient role in exhibiting the asymmetry in the mirror first-forbidden β -decays : $^{17}\text{Ne}(\beta^+)^{17}\text{F}$ and $^{17}\text{N}(\beta^-)^{17}\text{O}$.

This effect is independent of whether ZBM-F or ZBM-O effective interaction is used in describing β^- decay : $^{17}\text{N}(\beta^-)^{17}\text{O}$. The dashed line in Fig. 4 shows the dependence of

$(kI_0)^-$ and $(kaI_1 + kcI_2)^-$ on the parameter a of the first guess potential $U(r)$, which is calculated using the ZBM-F interaction, as in the calculation of $^{17}\text{Ne}(\beta^+)^{17}\text{F}$ decay rate. As before, $(kI_0)^-$ decreases strongly and $(kaI_1 + kcI_2)^-$ remains constant. This shows that the a -dependence of the ratio f^+/f^- is *not related* either to the choice of the particular variant of ZBM interaction or to the assumption of strict mirror symmetry in β^+ - and β^- - decays. On the other hand, the overall magnitude of this ratio depends strongly on the amount of mirror symmetry breaking in the many-body wave function. Replacing ZBM-O by ZBM-F in the calculation of $^{17}\text{N}(\beta^-)^{17}\text{O}$ decay rate, leads to the decrease of f^- by a factor ~ 1.8 (see also Fig. 4). This sensitivity, which has been stressed by Millener [5], is stronger than the a -dependence of f^- . The separate contributions of $(kaI_1)^\pm$, $(kbI_{-1})^\pm$, $(kcI_2)^\pm$ are given in Table 2. Nuclear matrix elements are shown in Table 3 for different SM interactions and SMEC radial wave functions. f^- is calculated for both ZBM-O and ZBM-F interactions. One can see that in the considered range of surface diffuseness parameters the enhancement rate of the ratio f^+/f^- is ~ 1.4 , independently of the assumption of strict mirror symmetry of the SM interaction.

In order to quantify the relative importance of radial sizes of the s.p. states and the mirror symmetry breaking in the many body wave functions, one has to constrain the surface diffuseness of the initial potential. Such a constraint can be provided by the proton radiative capture cross section $^{16}\text{O}(p, \gamma)^{17}\text{F}$ to the 'proton halo state' $1/2_1^+$, which is very sensitive to the size of $1s_{1/2}$ proton s.p. wave function [11,21]. The astrophysical S -factor as a function of the c.m. energy is shown in Fig. 5 for three values of the diffuseness parameter of the initial potential : $a = 0.4$ fm (the dotted line), 0.55 fm (the solid line) and 0.8 fm (the dashed line), separately for each decay branch : $^{16}\text{O}(p, \gamma)^{17}\text{F}(J^\pi = 1/2_1^+)$ and $^{16}\text{O}(p, \gamma)^{17}\text{F}(J^\pi = 5/2_1^+)$. One should notice that in all cases, energies of proton s.p. orbits $0d_{5/2}$ and $1s_{1/2}$ in the selfconsistent potentials for different a are at the experimental binding energies of $5/2_1^+$ and $1/2_1^+$ states in ^{17}F , respectively. The sum of contributions from these two decay branches is shown in the lower part of Fig. 5. The calculations are performed using SMEC wave functions (5) and (6) which have been obtained exactly in the same way and for exactly the same input parameters as those used in the calculation of both the decay rate $^{17}\text{Ne}(\beta^+)^{17}\text{F}$ (see Figs. 3 and 4) and the spectrum of ^{17}F (Fig. 1). The scale of excitation energy is the same as c.m. energy in the $p + ^{16}\text{O}$ system. The photon energy is given by the difference of c.m. energy of $[^{16}\text{O} + p]_{J_i^\pi}$ system and the experimental energy of the final state ($1/2_1^+$ or $5/2_1^+$) in ^{17}F . We have taken into account all possible $E1$, $E2$, and $M1$ transitions from incoming s , p , d , f , and g waves. It is clearly seen in Fig. 5 that the SMEC calculation for $a = 0.4$ fm underestimates the experimental capture cross-section. On the other hand, the calculation for $a = 0.8$ fm, for which the ratio f^+/f^- agrees with the data (see Fig. 3), overestimates strongly the data. Realistic values of the surface diffuseness parameter, which are compatible with the proton capture data [22], are : $a = 0.55 \pm 0.05$ fm. In this range, f^+ agrees perfectly with the experimental data, whereas f^- is too big. For $a = 0.55$ fm, f^- overshoots the data by a factor $\simeq 1.4$.

Since the radial dependences which are consistent with the proton capture reaction data, give excellent fit of both the β^+ -decay rate and the spectrum of ^{17}F , the discrepancy found for f^- and f^+/f^- should be explained by the deficiency of the effective SM interaction to reproduce the configuration mixing in ^{17}O (^{17}N). If one includes the effect of mirror symmetry breaking through the modification of energies of s.p. orbitals of the SM, then

the experimental value of f^- can be reproduced by SMEC wave function for $a = 0.55$ fm using : $\varepsilon_{d_{5/2}} = 3.21$ ($\varepsilon_{s_{1/2}} = 3.3$). For this interaction, called ZBM-O*, Fig. 6 shows SMEC energies and widths for positive parity (l.h.s. of the plot) and negative parity (r.h.s. of the plot) states of ^{17}O . Negative parity states are reproduced better by ZBM-O* than by ZBM-O SMEC calculations (*c.f.* Fig. 2 and Fig. 6). The splitting of $5/2_1^+$ and $1/2_1^+$ states in SMEC/ZBM-O* is slightly larger than the experimental splitting. The spacing $\varepsilon_{d_{5/2}} - \varepsilon_{s_{1/2}}$ in ZBM-O* is reduced too much as compared to ZBM-F interaction to account for the absence of the expected renormalization of the two-body matrix elements. Since the dominant configuration in $5/2_1^+$ and $1/2_1^+$ states is the 1p-0h component outside a closed core of ^{16}O with one nucleon in either $d_{5/2}$ or $s_{1/2}$ shells, therefore it is quite natural that the splitting $\varepsilon_{d_{5/2}} - \varepsilon_{s_{1/2}}$ in ZBM interaction has a particularly strong effect on the relative position of these two states.

An interesting supplementary quantity is the $B(E2)$ transition matrix element between $1/2_1^+$ and $5/2_1^+$ bound states of ^{17}F and ^{17}O . Assuming the effective charges : $e_p \equiv 1 + \delta_p$, $e_n \equiv \delta_n$, with the polarization charge $\delta = \delta_p = \delta_n = 0.2$, which are suggested by the theoretical estimates [23], one finds in SMEC/ZBM-F with $a = 0.55$ fm : $B(E2) = 74.85$ e²fm⁴ for ^{17}F . The experimental value for this transition is $B(E2)_{exp} = 64.92$ e²fm⁴. In ^{17}O one finds similar results : $B(E2) = 3$ and 3.2 e²fm⁴ in SMEC/ZBM-O and SMEC/ZBM-O* calculations, respectively. The experimental value for this transition is $B(E2)_{exp} = 6.2$ e²fm⁴.

Fig. 7 shows f^+ , f^- and f^+/f^- , which are calculated in SMEC for different values of the diffuseness parameter of the initial potential. The shaded areas give the experimental limits. f^+ and f^- are calculated with ZBM-F and ZBM-O* interactions, respectively. An essential physical parameter is the amplitude of a component ($1s_{1/2}^2 0p_{1/2}^{-1}$) in the g.s. wave functions of ^{17}Ne and ^{17}N . These amplitudes are shown in Table 4 together with the dominant 1p-0h component of the wave function in the final state $1/2_1^+$. One can notice that the amplitude of ($1s_{1/2}^2 0p_{1/2}^{-1}$) configuration in ^{17}Ne (ZBM-F) is $\sim 30\%$ bigger than in ^{17}N (ZBM-O*). One should however recall that this important difference concerns the small component of the wave function and the large component of the many-body wave function in the g.s. of ^{17}Ne and ^{17}N differs by less than 5%. The same change of the effective interaction induces only a small ($\sim 12\%$) difference of the dominant 1p-0h configuration in $1/2_1^+$ wave function of ^{17}F and ^{17}O .

In conclusion, we have found that the increase of the ratio f^+/f^- is correlated with the increase of radius of weakly bound $1s_{1/2}$ s.p. orbit in ^{17}F , in accordance with the conclusion of Borge et al. [3], but to obtain agreement with the data one has to assume an unrealistic geometry of the self-consistent potentials in ^{17}Ne , ^{17}N , ^{17}F and ^{17}O , which disagrees with the proton capture data. If, consistently, one takes into account the constraint from the capture data, one can estimate mirror symmetry breaking in the SM effective interaction in ZBM space for $A = 17$ nuclei. This effect is less than $\sim 5\%$ for the dominant term in the g.s. wave function and about $\sim 30\%$ for the small component of the wave function which plays a crucial role in the first-forbidden β -decay. In the final nucleus, the mirror symmetry breaking is less than $\sim 12\%$. These estimates are expected to depend somewhat on the SM space used. In particular, the absence of $0p_{3/2}$ and $0d_{3/2}$ subshells in the ZBM space may lead to the amplification of the sensitivity in the $1s_{1/2} \rightarrow 0p_{1/2}$ contribution to the charge-dependent effects [5].

Many nuclear matrix elements contribute to the transition probability so the experimental determination of the lifetime and spectrum shape alone is usually insufficient to determine them all. A unique first-forbidden β -transition from ^{17}N to the g.s. of ^{17}O is known ($f = 24 \pm 8$) [24]. Unfortunately, this transition tests the nuclear matrix element of rank 2 which are absent in the first-forbidden β -transition and which cannot be calculated reliably in a small effective SM space. SMEC gives for this unique first-forbidden transition a value which is ~ 3 times larger than the experimental value and depends weakly on the chosen hybrid of the ZBM force. This discrepancy is expected to be solved in calculations using large basis up to $4\hbar\omega$ [20,25]. Only in favourable circumstances, the nuclear structure information can be unambiguously extracted from the first-forbidden β -decays and relative importance of the configuration mixing (internal mixing) and the exotic radial dependences of s.p. wave functions (external mixing) can be disentangled. It seems that the first-forbidden β -decays, which depend sensitively both on the fine details of the SM effective interaction and on the radial formfactors of the wave functions in mirror systems will be particularly difficult to exploit as a direct and unambiguous source of information about unstable nuclei.

Acknowledgments

We thank the Institute for Nuclear Theory at the University of Washington for its hospitality and the Department of Energy for partial support during the completion of this work. It is a pleasure to thank G. Martínez-Pinedo for numerous discussions and to K. Langanke for valuable suggestions. This work was partly supported by KBN Grant No. 2 P03B 097 16 and the Grant No. 76044 of the French - Polish Cooperation.

REFERENCES

- [1] K. Bennaceur, F. Nowacki, J. Okołowicz, and M. Płoszajczak, *J. Phys.* **G 24** (1998) 1631.
- [2] K. Bennaceur, F. Nowacki, J. Okołowicz, and M. Płoszajczak, *Nucl. Phys.* **A 651** (1999) 289.
- [3] M.J.G. Borge, J. Deding, P.G. Hansen, B. Jonson, G. Martínez-Pinedo, P. Møller, G. Nyman, A. Poves, A. Richter, K. Riisager, O. Tengblad, *Phys. Lett.* **B 317** (1993) 25; G. Martínez-Pinedo, PhD thesis, Universidad Autónoma de Madrid.
- [4] A. Ozawa, M. Fujimaki, S. Fukuda, S. Ito, T. Kobayashi, S. Momota, T. Suzuki, I. Tanihata, K. Yoshida, G. Kraus and G. Münzenberg, *J. Phys. G: Nucl. Part. Phys.* **24** (1998) 143.
- [5] D.J. Millener, *Phys. Rev.* **C 55** (1997) R1633.
- [6] C. Mahaux and H.A. Weidenmüller, *Shell-model approach to nuclear reactions* (North-Holland, Amsterdam, 1969).
- [7] H.W. Bartz, I. Rotter, and J. Höhn, *Nucl. Phys.* **A 275** (1977) 111; *Nucl. Phys.* **A 307** (1977) 285; I. Rotter, *Rep. Prog. Phys.* **54** (1991) 635.
- [8] A.P. Zuker, B. Buck and J.B. McGrory, *Phys. Rev. Lett.* **21** (1968) 39.
- [9] A.P. Zuker, *Phys. Rev. Lett.* **23** (1969) 983.
- [10] K. Bennaceur, F. Nowacki, J. Okołowicz, and M. Płoszajczak, *Nucl. Phys.* **A 671** (2000) 203.
- [11] K. Bennaceur, N. Michel, F. Nowacki, J. Okołowicz, and M. Płoszajczak, *Phys. Lett.* **B 488** (2000) 75.
- [12] I.S. Towner and J.C. Hardy, *Nucl. Phys.* **A 179** (1972) 489.
- [13] D.J. Millener, D.E. Alburger, E.K. Warburton and D.H. Wilkinson, *Phys. Rev.* **C 26** 1167 (1982).
- [14] H. Schopper, *Weak Interactions and Nuclear Beta Decay* (North-Holland, Amsterdam, 1966).
- [15] D.H. Wilkinson, *Nuclear Physics with Heavy Ions and Mesons*, 1977, Les Houches Lectures, edited by R. Balian, M. Rho and G. Ripka (North-Holland, Amsterdam, 1978), p.955.
- [16] I.S. Towner, E.K. Warburton and G.T. Garvey, *Ann. Phys. (N.Y.)* **66** 674 (1971).
- [17] H. Behrens and W. Bühring, *Nucl. Phys.* **A 162** (1971) 111.
- [18] I.S. Towner and J.C. Hardy, in *"The Nucleus as a Laboratory for Studying Symmetries and Fundamental Interactions"*, eds. E.M. Henley and W.C. Haxton.
- [19] E.K. Warburton, *Phys. Rev.* **C 44** (1991) 233.
- [20] E.K. Warburton, I.S. Towner and B.A. Brown, *Phys. Rev.* **C 49** (1994) 824.
- [21] C. Rolfs, *Nucl. Phys.* **A 217** (1973) 29.
- [22] R. Morlock, R. Kunz, A. Mayer, M. Jaeger, A. Müller, J.W. Hammer, P. Mohr, H. Oberhummer, G. Staudt, and V. Kölle, *Phys. Rev. Lett.* **79** (1997) 3837.
- [23] M.W. Kirson, *Ann. Phys. (NY)* **82** (1974) 345.
- [24] M.G. Silbert and J.C. Hopkins **134** (1964) B16.
- [25] E.K. Warburton, B.A. Brown and D.J. Millener, *Phys. Lett.* **B 293** (1992) 7.

TABLES

TABLE I. The parameters of initial potentials $U(r)$ used in the calculations of self-consistent potentials $U^{(sc)}(r)$ for $s_{1/2}$ and $d_{5/2}$ s.p. wave functions in $1/2_1^+$ weakly bound state and $5/2^+$ ground state of ^{17}F , respectively. The residual coupling of Q and P subspaces is given by the DDSM1 interaction. For all considered cases the radius of the potential is $R_0 = 3.214$ fm. For more details, see the description in the text.

Diffuseness [fm]	V_0 [MeV]	V_{SO} [MeV]
0.40	-55.119	-1.383
0.45	-54.432	0.097
0.50	-53.6975	1.5185
0.55	-52.929	2.886
0.60	-52.139	4.203
0.65	-51.334	5.475
0.70	-50.521	6.706
0.75	-49.705	7.898
0.80	-48.889	9.054
0.85	-48.076	10.178

TABLE II. Nuclear matrix elements and decay rates are shown for different values of the diffuseness parameter of the 'first guess', initial potential $U(r)$. Quantities for β^+ -decays are calculated using ZBM-F interaction. For β^- -decay, ZBM-O, ZBM-O* and ZBM-F interactions are used.

Interaction	Matrix element	$a = 0.4$ fm	$a = 0.5$ fm	$a = 0.6$ fm	$a = 0.7$ fm	$a = 0.8$ fm
ZBM-F	$(kI_0)^+$	1024.88	872.67	718.37	584.54	483.76
	kaI_1^+	-5.10	-31.53	-72.23	-129.54	-205.88
	kbI_{-1}^+	1.60	1.62	1.67	1.76	1.88
	kcI_2^+	112.26	124.77	145.90	176.54	217.50
	$(kaI_1^+ + kcI_2^+)$	107.15	93.24	73.66	47.00	11.62
	f^+	1133.64	967.53	793.70	633.30	497.26
ZBM-O	$(kI_0)^-$	94.23	80.48	65.27	50.99	39.11
	kaI_1^-	-17.68	-18.32	-19.46	-21.13	-23.32
	kbI_{-1}^-	0.39	0.38	0.38	0.37	0.36
	kcI_2^-	4.46	5.04	5.99	7.35	9.185
	$(kaI_1^- + kcI_2^-)$	-13.28	-13.1	-13.47	-13.76	-14.13
	f^-	81.39	67.58	52.17	37.59	25.34
ZBM-O*	$(kI_0)^-$	66.01	56.355	45.69	35.72	27.5
	kaI_1^-	-13.475	-13.96	-14.83	-16.09	-17.755
	kbI_{-1}^-	0.29	0.285	0.28	0.27	0.26
	kcI_2^-	3.39	3.83	4.55	5.59	6.97
	$(kaI_1^- + kcI_2^-)$	-10.085	-10.13	-10.28	-10.5	-10.78
	f^-	56.215	46.51	35.69	25.49	16.98
ZBM-F	$(kI_0)^-$	165.015	141.02	114.46	89.40	68.36
	kaI_1^-	-27.94	-28.96	-30.77	-33.40	-36.88
	kbI_{-1}^-	0.64	0.63	0.62	0.605	0.585
	kcI_2^-	7.08	8.00	9.51	11.68	14.58
	$(kaI_1^- + kcI_2^-)$	-20.86	-20.95	-21.25	-21.72	-22.29
	f^-	144.80	120.70	93.82	68.29	46.65

TABLE III. Nuclear matrix elements for different values of the diffuseness parameter of the initial potential $U(r)$. Quantities for β^+ -decays are calculated using ZBM-F interaction. For β^- -decay, ZBM-O, ZBM-O* and ZBM-F interactions are used.

Quantity	Matrix element	$a = 0.4$	$a = 0.5$	$a = 0.6$	$a = 0.7$	$a = 0.8$
f^+ (ZBM-F)	$\xi'v$	24.05	22.62	21.03	19.43	17.89
	$\xi'y$	-8.44	-7.93	-7.36	-6.78	-6.21
	w	-0.53	-0.56	-0.60	-0.67	-0.74
	w'	-0.40	-0.41	-0.43	-0.46	-0.49
	u	0.63	0.66	0.72	0.79	0.88
	u'	0.47	0.485	0.51	0.54	0.58
	x	-0.20	-0.21	-0.22	-0.25	-0.27
	x'	-0.15	-0.15	-0.16	-0.17	-0.18
f^- (ZBM-O)	$\xi'v$	-19.36	-18.17	-16.74	-15.19	-13.62
	$\xi'y$	-7.06	-6.63	-6.12	-5.57	-5.02
	w	0.48	0.51	0.56	0.62	0.69
	w'	0.37	0.38	0.40	0.43	0.47
	u	-0.56	-0.60	-0.65	-0.72	-0.81
	u'	-0.43	-0.45	-0.47	-0.51	-0.55
	x	-0.18	-0.19	-0.21	-0.235	-0.26
	x'	-0.14	-0.14	-0.15	-0.17	-0.18
f^- (ZBM-O*)	$\xi'v$	-16.2	-15.21	-14.0	-12.7	-11.38
	$\xi'y$	-6.17	-5.8	-5.35	-4.87	-4.385
	w	0.42	0.45	0.49	0.54	0.61
	w'	0.32	0.335	0.355	0.38	0.41
	u	-0.49	-0.52	-0.57	-0.63	-0.705
	u'	-0.37	-0.39	-0.41	-0.44	-0.48
	x	-0.16	-0.17	-0.18	-0.2	-0.22
	x'	-0.12	-0.12	-0.13	-0.14	-0.15
f^- (ZBM-F)	$\xi'v$	-25.61	-24.05	-22.16	-20.12	-18.05
	$\xi'y$	-8.87	-8.33	-7.69	-7.00	-6.30
	w	0.60	0.64	0.695	0.77	0.86
	w'	0.46	0.475	0.50	0.54	0.59
	u	-0.71	-0.75	-0.82	-0.91	-1.02
	u'	-0.54	-0.56	-0.60	-0.64	-0.69
	x	-0.235	-0.25	-0.27	-0.30	-0.34
	x'	-0.18	-0.19	-0.20	-0.21	-0.23

TABLE IV. The amplitudes of components $(1s_{1/2}^2 0p_{1/2}^{-1})$, $(0d_{1/2}^2 0p_{1/2}^{-1})$ in the initial state $1/2_1^-$ of the β^+/β^- decay of $^{17}\text{Ne}/^{17}\text{N}$ and the dominant components $1s_{1/2}$ and $0d_{5/2}$ in the final first excited state $1/2_1^+$ and in the g.s. of $^{17}\text{F}/^{17}\text{O}$, respectively, for different hybrids of the ZBM interaction.

Interaction	$(1s_{1/2}^2 0p_{1/2}^{-1})^{J^\pi=1/2_1^-}$	$(0d_{5/2}^2 0p_{1/2}^{-1})^{J^\pi=1/2_1^-}$	$(1s_{1/2})^{J^\pi=1/2_1^+}$	$(0d_{5/2})^{J^\pi=5/2_1^+}$
ZBM [8]	0.41	0.758	0.65	0.69
ZBM-F	0.399	0.78	0.665	0.707
ZBM-O	0.311	0.80	0.62	0.667
ZBM-O*	0.268	0.81	0.587	0.637

FIGURES

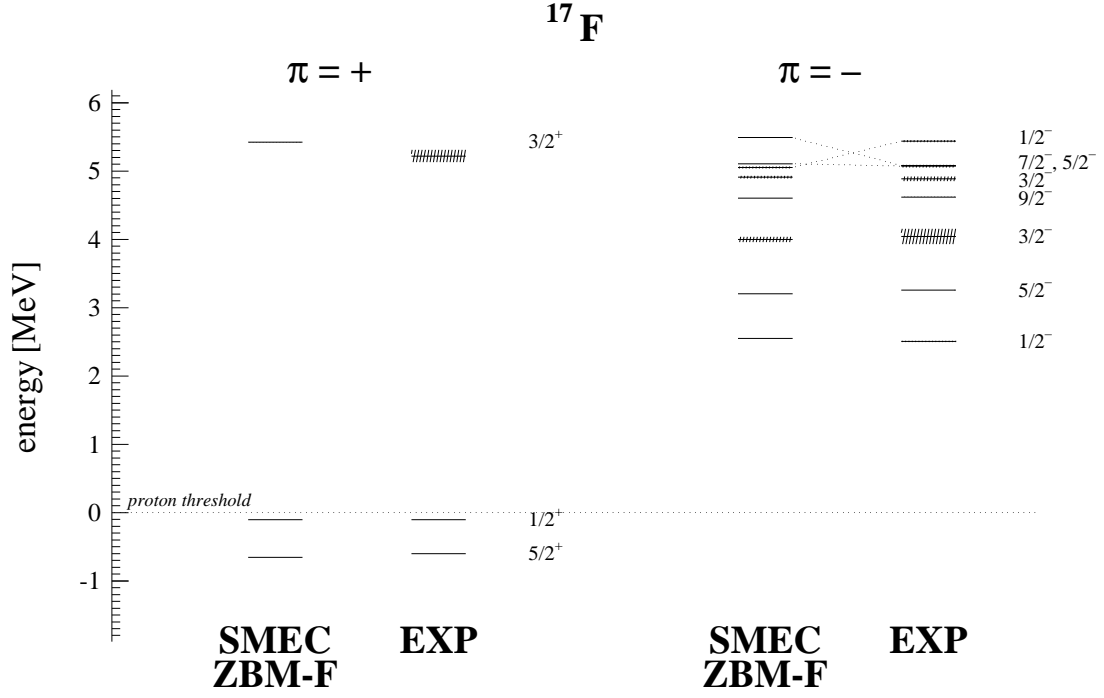


FIG. 1. Comparison of experimental spectrum of ^{17}F with the spectrum calculated using SMEC with the ZBM-F effective interaction. Residual coupling to the continuum state is provided by the density dependent DDSM1 interaction [10]. The proton threshold energy is adjusted to reproduce position of the $1/2_1^+$ first excited state. The shaded regions represent the width of resonance states.

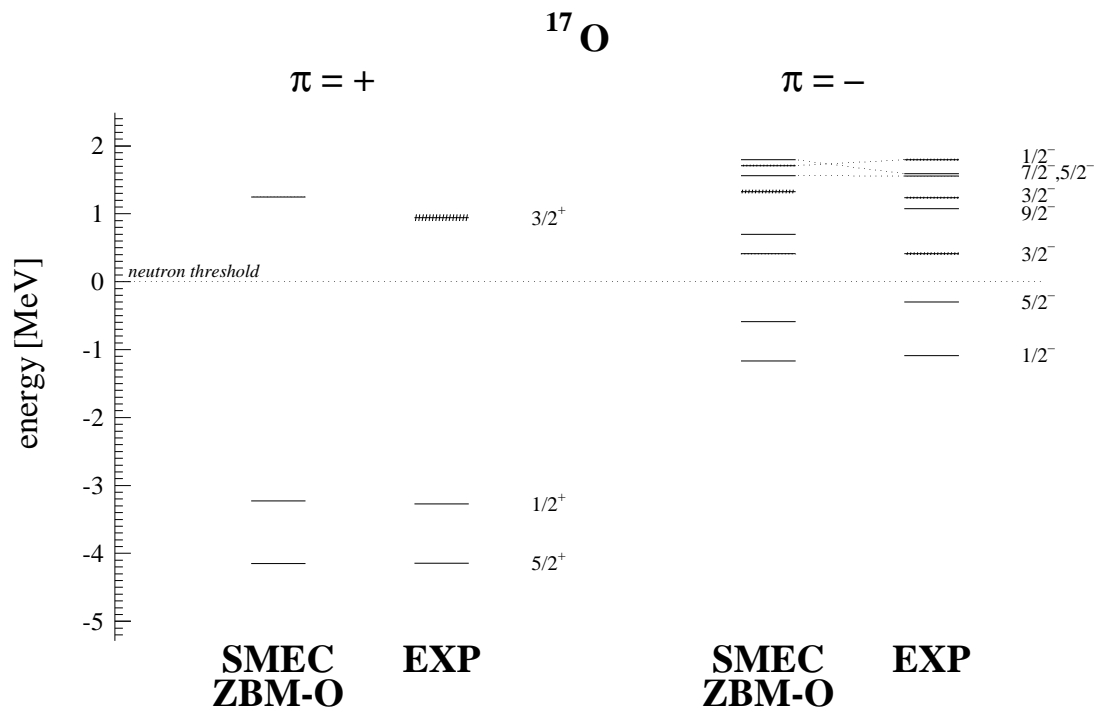


FIG. 2. The same as in Fig. 1 but for ^{17}O . The neutron threshold energy is adjusted to reproduce position of the first $3/2_1^-$ excited state.

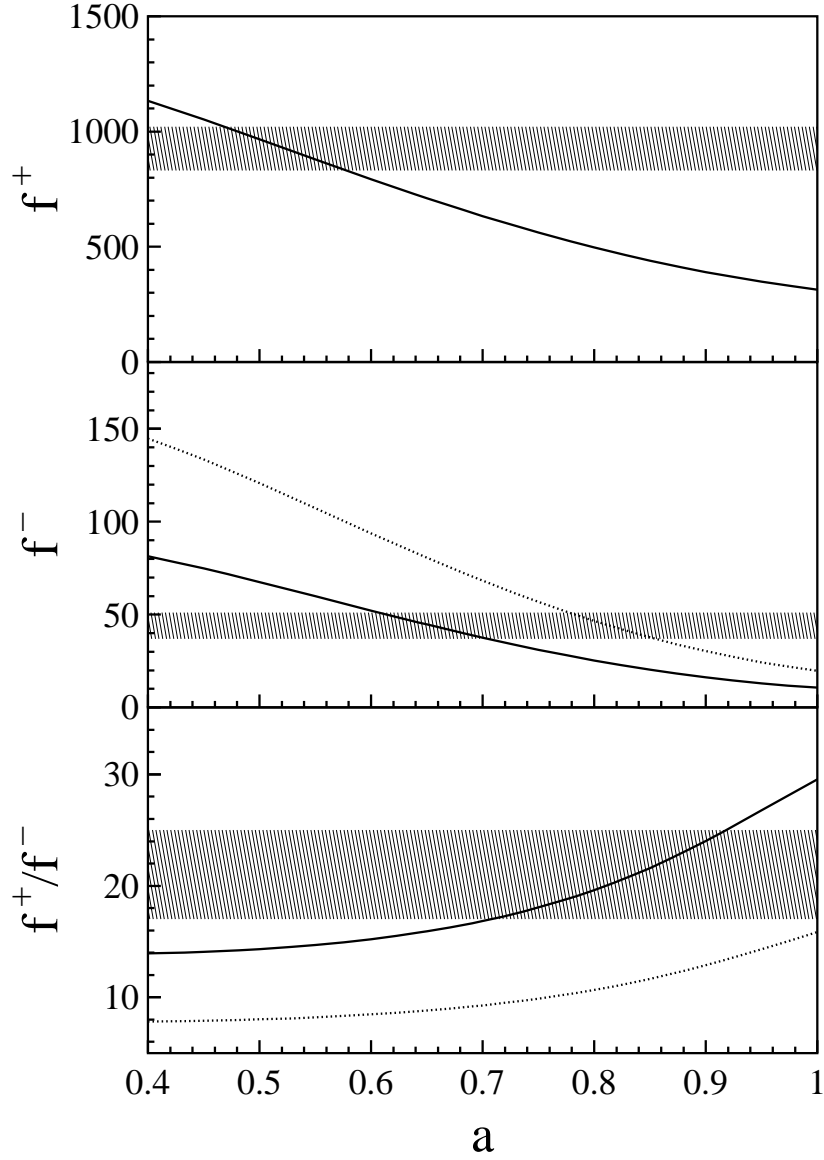


FIG. 3. f^+ , f^- values and the ratio f^+/f^- for the first-forbidden β -transitions from the ground states of ^{17}Ne and ^{17}N , are calculated using SMEC for different values of the diffuseness a of the initial average potential. Calculations are performed in the ZBM space using the DDSM1 residual interaction. The shaded areas show experimental uncertainty for f^+ , f^- and f^+/f^- , respectively. The dotted line corresponds to the mirror symmetric SMEC calculations for $^{17}\text{Ne}(\beta^+)^{17}\text{F}$ and $^{17}\text{N}(\beta^-)^{17}\text{O}$ using in both cases the ZBM-F effective interaction.

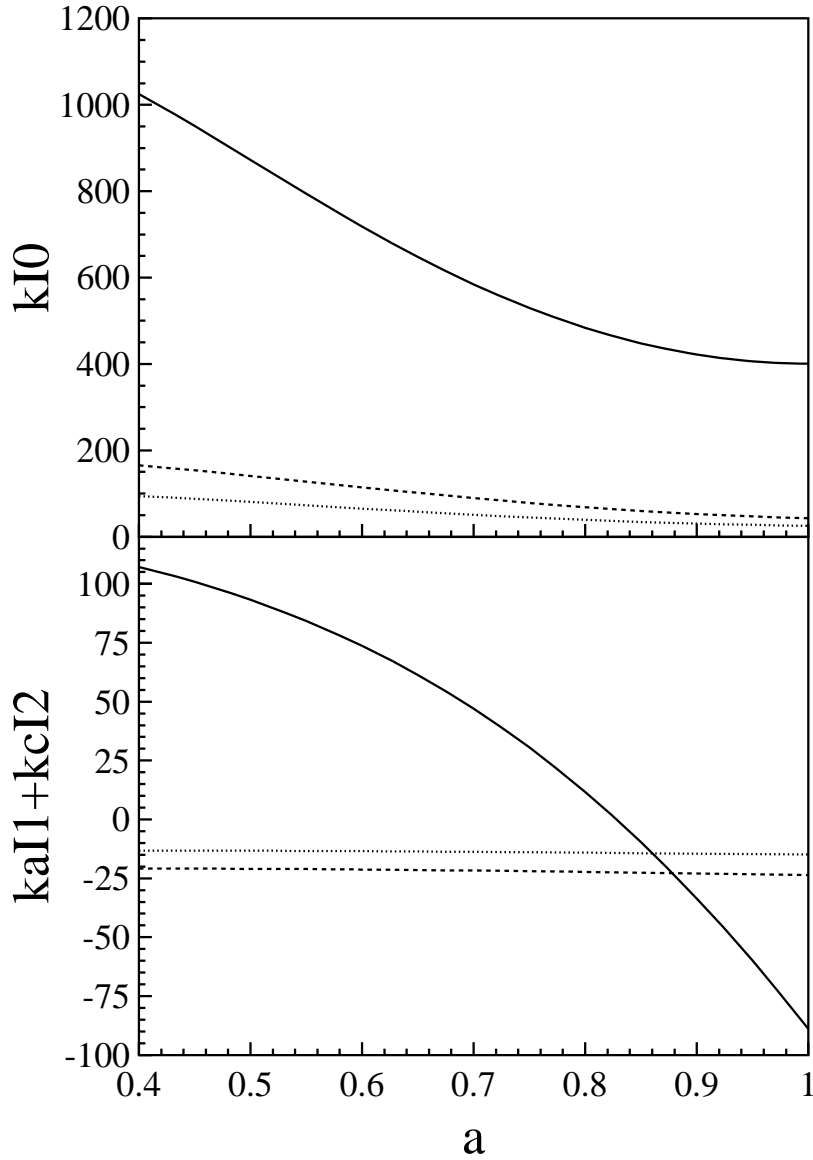


FIG. 4. Nuclear matrix elements kI_0 (upper part) and $(kaI_1 + kcI_2)$ (lower part) are plotted as a function of the diffuseness of the 'first guess' initial average potential. Calculations are performed in the ZBM space using the DDSM1 residual interaction. The solid line shows the matrix elements for the transition $^{17}\text{Ne}(\beta^+)^{17}\text{F}$ which is calculated using the ZBM-F interaction. The dashed and dotted lines show the matrix elements for the transition $^{17}\text{N}(\beta^-)^{17}\text{O}$ calculated using ZBM-F and ZBM-O interactions, respectively.

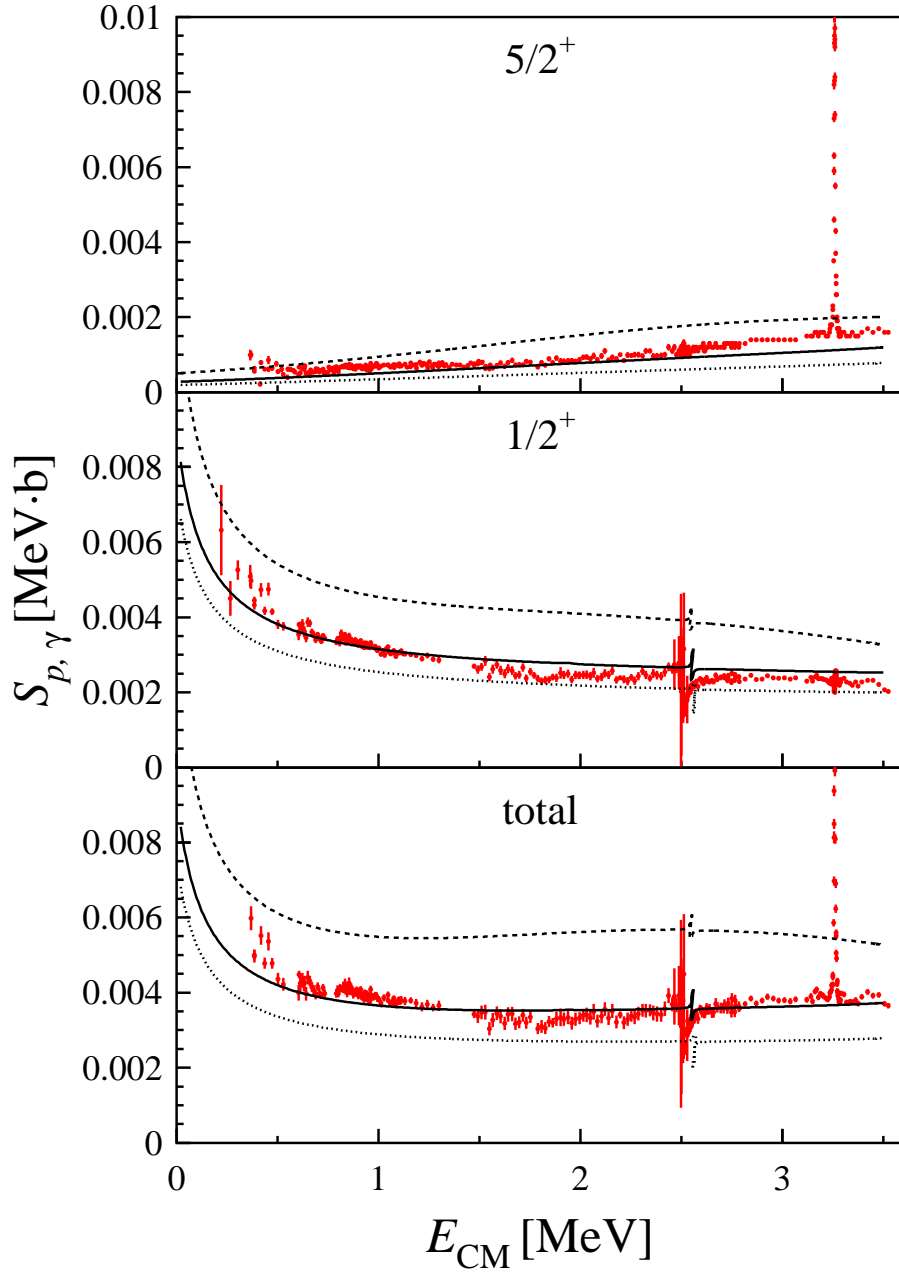


FIG. 5. The astrophysical S -factor for the reactions $^{16}\text{O}(p,\gamma)^{17}\text{F}(J^\pi = 5/2_1^+)$ and $^{16}\text{O}(p,\gamma)^{17}\text{F}(J^\pi = 1/2_1^+)$, is plotted as a function of the center of mass energy E_{CM} for three different values of the diffuseness of the initial (auxiliary) potential : $a = 0.4$ fm (the dotted line), $a = 0.55$ fm (the solid line) and $a = 0.8$ fm (the dashed line). The experimental data are taken from Ref. [22].

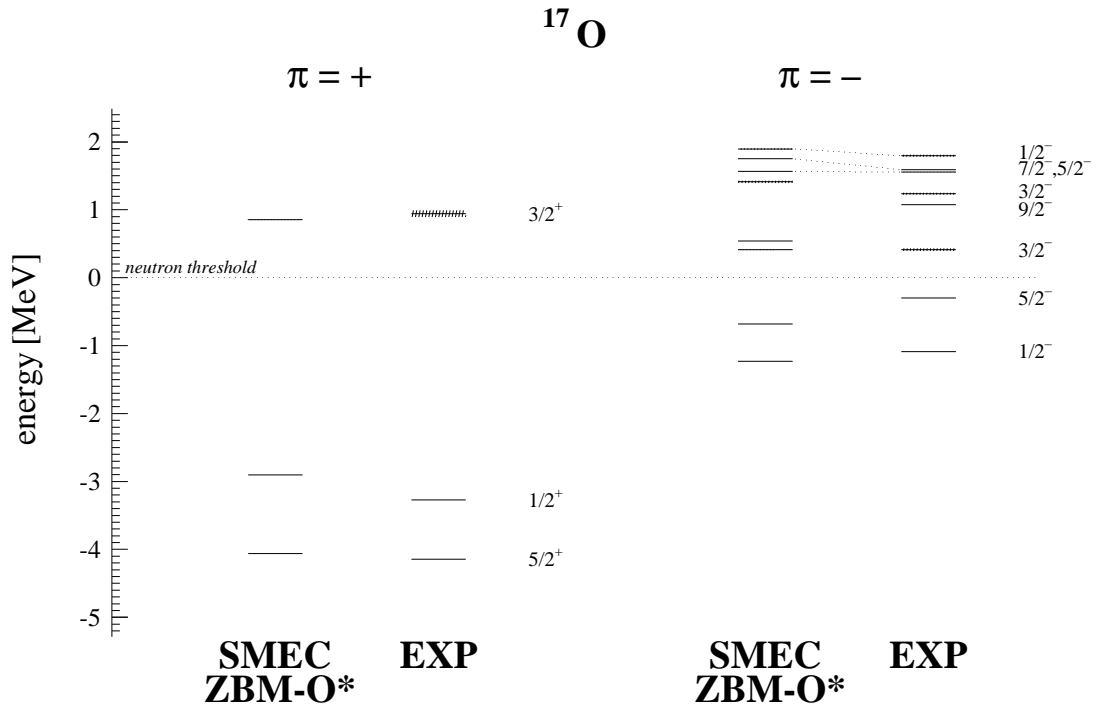


FIG. 6. The same as in Fig. 2 but for ZBM-O* effective interaction which yields the correct value for the β^- first-forbidden decay rate of ^{17}N in the ground state. The neutron threshold energy is adjusted to reproduce position of the first $3/2_1^-$ excited state.

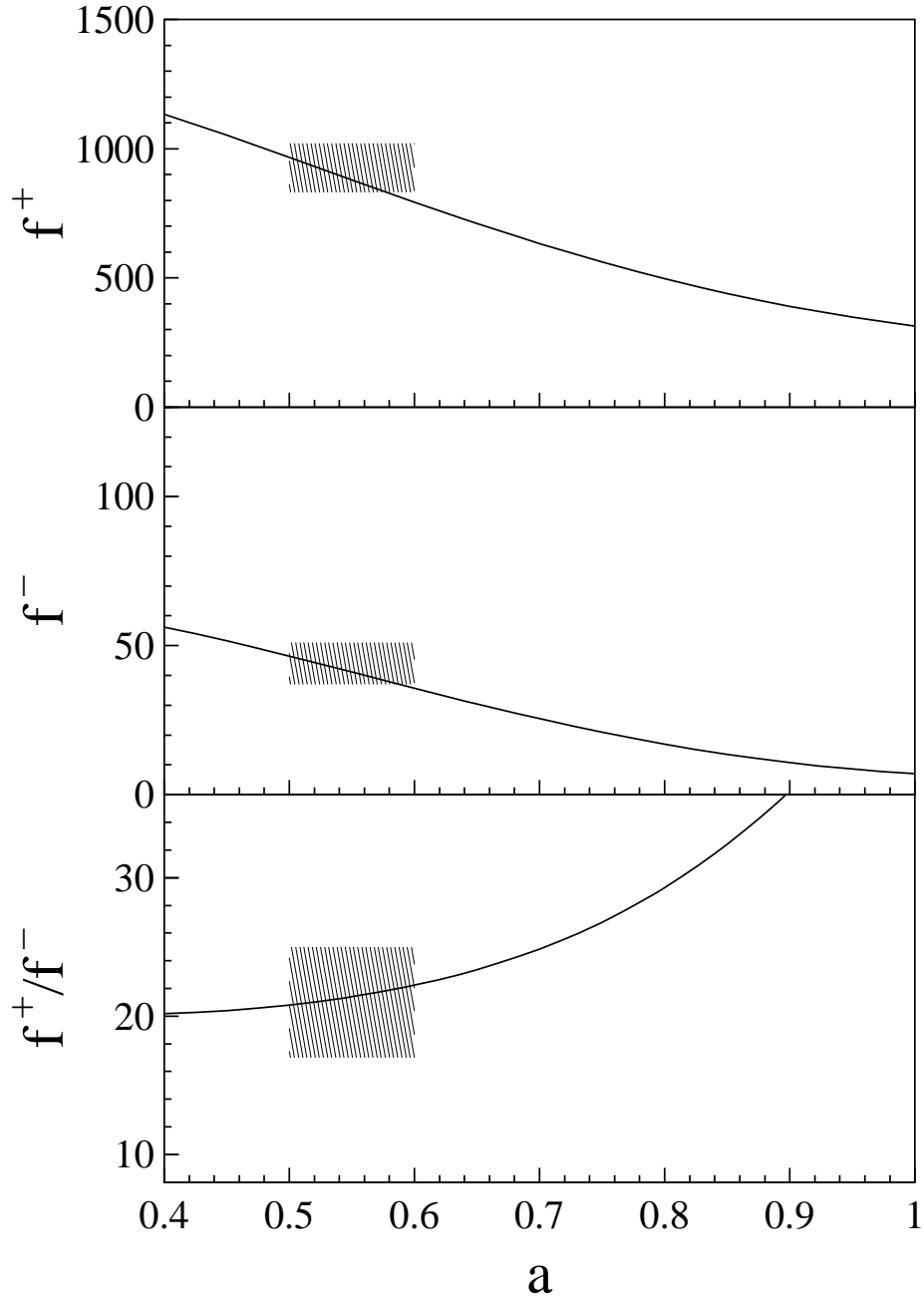


FIG. 7. f^+ , f^- values and the ratio f^+/f^- for the first-forbidden transitions from the ground states of ^{17}Ne and ^{17}N , are calculated using SMEC for different initial values of the diffuseness of the initial average potential. ZBM-O* effective shell model interaction is used to calculate the structure of ^{17}O . For more details, see the description in the text and the caption of Fig. 3.